AD-A260 275

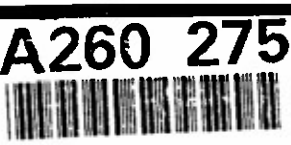

CUMENTATION PAGE

Form Approved
OMB No. 0704-0188

(2)

nation is estimated to average 1 hour per response, including the time for reviewing instructions, searching existing data sources, completing and reviewing the collection of information. Send comments regarding this burden estimate or any other aspect of this reducing this burden, to Washington Headquarters Services, Directorate for information Operations and Reports, 1215 Jefferson 02, and to the Office of Management and Budget, Paperwork Reduction Project (0704-0188), Washington, DC 20503.

2. REPORT DATE	3. REPORT TYPE AND DATES COVERED
12/29/92	Final 17 Sep 89 - 17 Sep 92

4. TITLE AND SUBTITLE
OPTICAL STUDIES OF LATERALLY CONFINED QUANTUM WELL STRUCTURES GROWN ON EX-SITU AND IN-SITU PATTERNED SUBSTRATES

5. FUNDING NUMBERS
DAAL03-89-K-0170

6. AUTHOR(S)
ANUPAM MADHUKAR

7. PERFORMING ORGANIZATION NAME(S) AND ADDRESS(ES)
UNIVERSITY OF SOUTHERN CALIFORNIA
MATERIALS SCIENCE AND ENGINEERING
UNIVERSITY PARK, VHE 506
LOS ANGELES, CA 90089-0241

8. PERFORMING ORGANIZATION REPORT NUMBER

9. SPONSORING/MONITORING AGENCY NAME(S) AND ADDRESS(ES)
U. S. Army Research Office
P. O. Box 12211
Research Triangle Park, NC 27709-2211

10. SPONSORING/MONITORING AGENCY REPORT NUMBER
ARO 27298.1-EL

11. SUPPLEMENTARY NOTES
The view, opinions and/or findings contained in this report are those of the author(s) and should not be construed as an official Department of the Army position, policy, or decision, unless so designated by other documentation.

12a. DISTRIBUTION/AVAILABILITY STATEMENT
Approved for public relesse; distribution unlimited.

12b. DISTRIBUTION CODE

13. ABSTRACT *(Maximum 200 words)*

This final technical report on ARO Contract No. DAAL03-89-K-0170 summarizes the issues examined and the findings related to (1) absorption and electroabsorption behavior of strained GaAs/InGaAs multiple quantum wells (MQW), (2) the dc transport characteristics of strained GaAs/InGaAs/AlAs based resonant tunnelling diodes, and (3) realization of three-dimensionally confined quantum well structures on patterned GaAs(111)B substrates via a one-step growth process labelled substrate encoded sized reducing epitaxy (SESRE). Use of pre-patterned substrates as a means of strain relief without the generation of dislocations is shown to allow growth of high quality MQWs to thicknesses of ≈1μm needed for sufficient optical interaction path length in p-i(MQW)-n modulators and detectors. The role of defect induced deep levels in impacting the exciton linewidth through their influence on the internal field distribution is revealed for the first time. Three dimensionally confined GaAs/AlGaAs structures are realized for the first time using SESRE.

14. SUBJECT TERMS	15. NUMBER OF PAGES
STRAINED QUANTUM WELLS, DEFECT REDUCTION, PATTERNED SUBSTRATES, ELECTROABSORPTION, MODULATORS, RESONANT TUNNELLING DIODES, LATERAL CONFINEMENT, QUANTUM BOX, GaAs(100)/InGaAs,GaAs(111)B/AlGaAs.	TWENTY EIGHT
	16. PRICE CODE

17. SECURITY CLASSIFICATION OF REPORT	18. SECURITY CLASSIFICATION OF THIS PAGE	19. SECURITY CLASSIFICATION OF ABSTRACT	20. LIMITATION OF ABSTRACT
UNCLASSIFIED	UNCLASSIFIED	UNCLASSIFIED	UL

OPTICAL STUDIES OF LATERALLY CONFINED QUANTUM WELL STRUCTURES GROWN ON EX-SITU AND IN-SITU PATTERNED SUBSTRATES

FINAL REPORT

AUTHOR: PROFESSOR ANUPAM MADHUKAR

DECEMBER 28, 1992

SUBMITTED TO:
ARMY RESEARCH OFFICE
P.O. BOX 12221
RESEARCH TRIANGLE PARK
NORTH CAROLINA, 27709-2211
ATTN: DR. JOHN ZAVADA

CONTRACT NO. DAALO3-89-K-0170

SUBMITTED BY:
DEPARTMENT OF MATERIALS SCIENCE & ENGINEERING
UNIVERSITY OF SOUTHERN CALIFORNIA
LOS ANGELES, CA 90089-0241
(213) 740-4325

APPROVED FOR PUBLIC RELEASE;
DISTRIBUTION UNLIMITED.

TABLE OF CONTENTS

FOREWARD

This final technical report on ARO Contract No. DAAL03-89-K-0170 provides a summary of the salient accomplishments during the contract period. As required, it also lists the graduate students supported by the contract and the publications resulting from the work supported by this contract.

I LIST OF ILLUSTRATIONS

II. OBJECTIVES AND SCOPE:

The objectives of the contract were to examine the optical and vertical transport properties of III-V semiconductor structures of relevance to optoelectronic applications and grown on pre-patterned substrates. The scope of the work was limited to (1) examining the consequences for the optical and vertical transport behavior of growth of the strained InGaAs/AlGaAs single and multiple quantum well structures on unpatterned and pre-patterned GaAs(100) substrates with the objective of realizing strain relief without defect generation and (2) the growth of the lattice matched GaAs/AlGaAs system on unpatterned and pre-patterned GaAs(111)B with the objective of examining the potential of a one-step growth control approach to the realization of three-dimensionally confined structures. Accordingly, the technical summary that follows is divided into the three categories of,

:Optical studies of InGaAs/AlGaAs on unpatterned and pre-patterned GaAs(100)

:Transport behavior of InGaAs/AlGaAs resonant tunnelling diodes on unpatterned and patterned GaAs(100)

:GaAs/AlGaAs growth on unpatterned and patterned GaAs(111)B.

III. SUMMARY OF SALIENT ACCOMPLISHMENTS:

III.A OPTICAL STUDIES OF STRAINED GROWTH ON UNPATTERNED AND PATTERNED SUBSTRATES

The optical behavior of the strained InGaAs/AlGaAs single and multiple quantum wells grown on GaAs(100) substrates offers (1) an ideal test system for examining fundamental aspects of the role of strain in epitaxy and possible approaches to minimizing strain induced defects via alternative means of strain relief, and (2) a system of considerable technological significance to GaAs based optoelectronic and electronic technology for applications in optical communication, information processing, computing and high speed/high power electronics. Its potential for the latter, however, depends upon establishing the limits on material quality and device structures capable of delivering the performance capability demanded. Such limits arise from inherent features of strained growth and the inevitable formation of defects deleterious to the material properties upon which rests the device performance. Defect formation is an inevitable consequence of the need to relieve the increasing strain energy with increasing thickness of the strained layer system for a given lattice mismatch. For applications in electro-absorption or electro-refraction based modulators and detectors, the active device layer thickness generally needed is ~1μm to achieve the required optical interaction path length. Such thicknesses are generally significantly beyond the so-called critical layer thickness for defect (dislocation) generation for the In compositions demanded by the operating wavelength (e.g. 0.98μm

wavelength corresponding to the E_r-doped optical fibers requires In compositions near 20% with an attendant strain of ~1.8% and a critical thickness estimated to vary between 130Å to 550Å[1-3]). Thus alternative means of achieving strain relief are required. Growth on pre-patterned mesas offers such an approach and the focus of the studies undertaken under this contract was to uncover the limits and trade-offs involved.

To this end, we undertook comparative studies of the optical absorption and electro-absorption behavior of InGaAs/AlGaAs single and multiple quantum wells grown on GaAs(100) unpatterned and patterned substrates over a range of (i) In and Al compositions, (ii) individual and multilayer thicknesses, (iii) the kinetics attendant to the growth conditions, and (iv) the size and nature of the patterned mesas. Although the scope of the work within the resources provided by this contract was limited primarily to studies of the optical behavior, naturally an understanding of the why of the observations demanded examining the nature and the density of dislocations and other deleterious defects and establishing connections between the optical behavior, the nature and density of defects, and the growth conditions. Fortunately, studies of the defects via high resolution electron microscopy were sponsored during an overlapping time period by the Office of Naval Research and indeed the focus on optical studies under this ARO contract was chosen for both its intrinsic value and complementary nature to the defect studies, the synergism between the two leveraging the investments of each. The completeness of scientific presentation demands that the salient accomplishments summarized below not only note the results of the optical studies but also relate them to the knowledge gained from the structural studies. We have thus followed this integrated scientific approach but it is to be clearly recognized that the resources of this contract were focused on the optical studies.

III.A1 Optical Behavior and Defect Reduction via Growth on pre-patterned GaAs(100)

It has been recognized that the efficiency of multiple quantum wells (MQW) as the active material in quantum confined Stark effect (QCSE) based light modulators depends on (1) the shift of the first electron-heavy hole excitonic transition per unit drive voltage, (2) the linewidth of the exciton with and without external bias, and (3) the rate of oscillator strength decrease with increasing bias. These factors have been considered in optimizing the **lattice matched** (i.e. unstrained) GaAs/AlGaAs MQW structures for electro-absorption modulators[4,5]. Additional considerations are required for optimizing the **lattice mismatched** InGaAs/GaAs MQWs for use in light modulators because of the following reasons: 1) The lattice mismatch between InGaAs and GaAs causes degradation of the growth front, defect generation beyond a critical thickness for a given In content, and the tendency for three dimensional growth mode. These impose limitations on the choice of the InGaAs layer thickness and In composition. 2) Since the well

layer, where most of the wavefunction resides, is an alloy (InGaAs), the alloy scattering plays a role in determining the exciton linewidth dependence on the well width.

:Unpatterned Substrates

Motivated by the above considerations, we at first carried out systematic studies of the electro-absorption behavior of $In_xGa_{1-x}As/GaAs$ single quantum wells (SQWs) and MQWs in order to examine 1) the relation between the exciton linewidth and the well width for various In compositions in the MQWs, and 2) the minimum barrier width required to effectively isolate the quantum wells (QW).

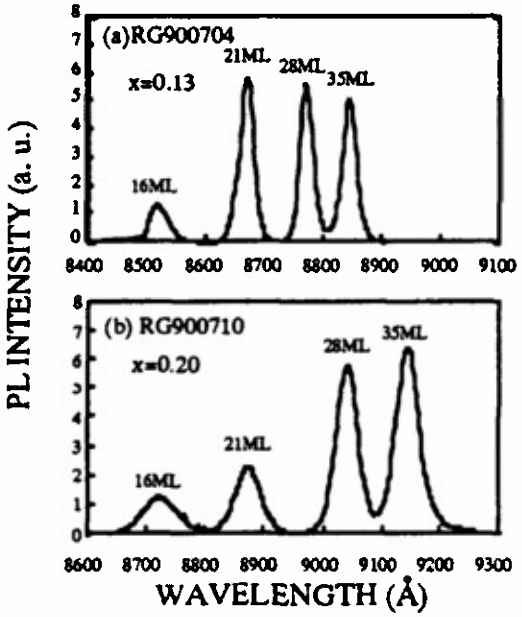

Fig. 1 5K photoluminesecence from (a) sample RG900704 and (b) sample RG 900710.

Figs. 1 (a) and (b) show the 5K PL results on two typical samples (RG900704 and RG900710), each containing four SQW of well widths 16 monolayer (ML), 21ML, 28ML and 35ML and In content 0.13 and 0.20, respectively. They were chosen to cover the range of practical value to quantum confined Stark effect (QCSE) devices and to be distributed evenly in both well width and exciton transition energy range. The growth sequence is thin well to thick well in order to minimize the possibility of dislocations generated in one well from propagating into the subsequent wells. Very thick GaAs barriers of 180ML were grown between the SQWs to prohibit electronic communication between the wells. Such thickness is also found through reflection high energy electron diffraction (RHEED) studies to be adequate for recovering the surface to the same condition as the starting point of the previous wells.

In the PL measurements, the excitation energy of a Ti-sapphire laser was tuned at 8450Å, slightly below the GaAs bandgap and above all the exciton transition energies of interest. The excitation power was varied from $0.01W/cm^2$ to $10W/cm^2$. The peaks are quite symmetric and remain unshifted under all excitation powers, indicating the excitonic nature of these transitions. The PL is found to be very efficient and is estimated to be 1 to 2 orders of magnitude more efficient than that from $GaAs/Al_{0.3}Ga_{0.7}As$ SQW samples. Unlike the GaAs/AlGaAs QWs in which the exciton PL intensity is found to increase linearly or superlinearly with increasing power[6], it is found to increase sublinearly with increasing power in these InGaAs/GaAs samples.

The linewidths remain almost constant for excitation power $\leq$ 1W/cm^2 and start to increase beyond 1W/cm^2, the behavior near the exciton tail changing faster than that at half maximum. These linewidths were generally amongst the narrowest found in the literature at the time. Note that there exists a minimum linewidth in the well width range studied. For the x = 0.13 sample (RG900704), this minimum linewidth is found to lie in a rather wide region, between 28 ML and 35 ML. This exciton linewidth minimum behavior becomes more evident at higher In composition as seen in sample RG 900710 (x = 0.20) where the minimum is located at 28 ML. This behavior is different from the linewidth - well width relation previously reported for the GaAs/AlGaAs[7,8] and the InGaAs/GaAs systems[7]. The minimum linewidth of 4.2 meV for the x = 0.13 sample and 6.2 meV for the x = 0.20 sample is found to satisfy the x(1-x) rule closely, indicating that the alloy scattering contributes an important factor to the linewidth in this class of samples. This phenomenon can be understood by taking into account the interfacial and alloy scattering, as well as the possible degradation in growth front for thicker InGaAs layers[9].

Guided by the above noted findings on SQWs, we grew appropriate MQWs and examined their behavior with a particular eye towards their use in electroabsorptive modulators. In order to maximize the efficiency of the MQW, i.e. maximum absorption change per unit external bias, it is necessary to minimize the QW barrier thickness. This is particularly important for a MQW placed inside an asymmetric Fabry-Perot (FP) cavity since the FP mode wavelength is sensitive to the thickness of the cavity and thus the growth nonuniformity across the sample. The barrier width can be reduced to a minimum thickness sufficient for isolating the wells without compromising the electro-absorption behavior. We calculated the minimum barrier widths by considering the MQW as a superlattice and determining the barrier width for a given x and well width such that the width of the superlattice miniband is one order of magnitude smaller than the room temperature FWHM of the excitonic feature in a good quality MQW. MQWs with barrier widths $\geq$ this critical value were grown and their absorption behavior and electro-absorption behavior measured and compared on a per well basis. Fig. 2 shows the absolute value of the maximum

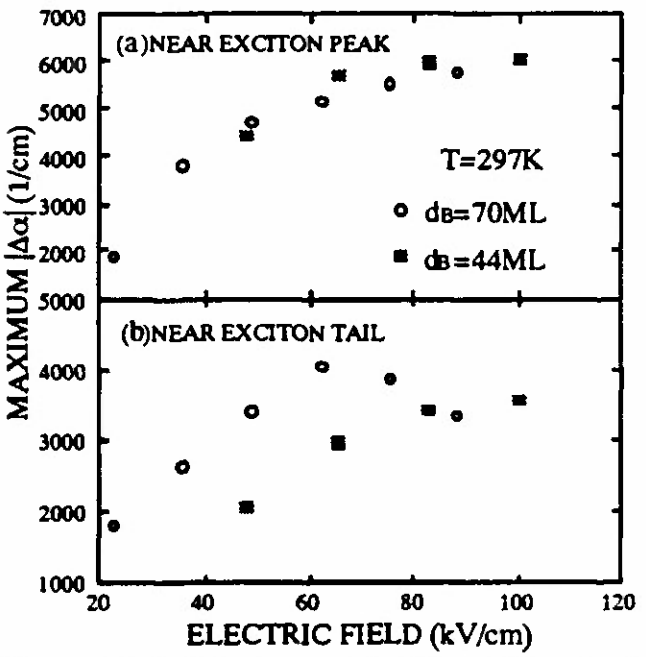

Fig.2 Comparison of the maximum change in the absorption coefficient as a function of applied electric field for InGaAs/GaAs MQW with 70 ML and 44 ML barrier width.

change in the absorption coefficient ($|\Delta\alpha|_{max}$), (a) near the exciton peak and (b) in the exciton tail region for sample RG900420, a 50 period MQW p-i-n structure with 35ML wide $In_{0.11}Ga_{0.89}As$ wells and 70ML wide GaAs barriers and sample RG900802, a similar structure with $In_{0.13}Ga_{0.87}As$ wells but reduced barrier width of 44ML. The In compositions across the 2cm x 2cm wafer for these samples are 0.11±0.01 and 0.13±0.01, respectively. For proper normalization, the absorption coefficient is extracted by accounting for only the total thickness of the active well layers and the electric field is extracted by taking into account the built-in electric field. While no significant difference was found in these two samples at zero bias, the $|\Delta\alpha|_{max}$ for sample RG900802 is slightly larger near the exciton peak but smaller in the exciton tail region, possibly due to the faster reduction in oscillator strength under bias for thinner barriers.

As an increase in the well depth via introduction of Al in the barriers and/or increase in the In content in the well provides a trade-off between the exciton linewidth, the absolute oscillator strength, the rate of shift of the exciton position with applied bias, and the rate of oscillator strength decay, we also examined the behavior of $Al_yGa_{1-y}Al$ / $In_xGa_{1-x}As$ / $Al_zGa_{1-z}As$ symmetric (y=z) and asymmetric (y≠z) SQWs. We succeeded in growing high quality single quantum wells in the highly strained $Al_xGa_{1-x}As$ / $In_{0.26}Ga_{0.74}As$ / $Al_zGa_{1-z}As$ system with $0 \leq x, z \leq 1.0$, using RHEED oscillation behaviour[10] as a guide for finding optimised regimes of growth conditions. Photoluminescence linewidths of 5 to 6 meV for $0.30 \leq x, z \leq 0.70$ were achieved. These results have set the stage for growth of high In and Al bearing strained MQWs with the high quality needed for their use in electroabsorptive or electrorefractive asymmetric FP modulators.

The above noted finding were reported in publications 1,2 and 3 noted in sec.IV.

:Patterned Substrates

Having arrived at a reasonably good behavior of MQW absorption and electro-absorption characteristics permitted by growth on **unpatterned** substrates, we next examined the possibility of improved behavior through growth on **pre-patterned** GaAs(100) mesas. To establish bounds on the advantage to be had we examined growth of single $In_xGa_{1-x}As$ layers and InGaAs/GaAs MQWs as a function of (i) x up to 0.25 and (ii) the growth conditions, on GaAs(100) substrates having mesas in the form of long ridges with widths down to submicron regime, as well as mesas of rectangular shapes with linear dimensions down to ~10 μm.

The GaAs(100) substrates were patterened using conventional optical lithography and wet chemical etching. For the studies aimed at establishing the limits of the advantages to be had in terms of maximum individual layer thicknesses, parallel sets of narrow mesas aligned along the [011] direction were employed. This choice was made to eliminate complications arising from significant interfacet migration effects found for growth on mesas aligned along [0$\bar{1}$1] even

for lattice-matched systems[11]. Patterning etches were carried out in a solution of $NH_4OH:H_2O_2:H_2O(1:1:5)$ and a final free etch was carried out in $NH_4OH:H_2O_2:H_2O(4:1:20)$ prior to loading the sample into the growth chamber. Substrates contained both patterned and unpatterned regions in order to compare the effects of patterning within the same growth. A 25Å $Al_{0.5}Ga_{0.5}As$ marker layer was laid down immediately following oxide desorption from the substrate so as to delineate the precise profile of the starting pattern. The arsenic pressure was kept at about 30% higher than the critical pressure required to maintain an As-stabilized (2x4) surface. The transmission electron microscopy (TEM) specimen were made from within 3mms of one another to eliminate any compositional variations arising from flux nonuniformity.

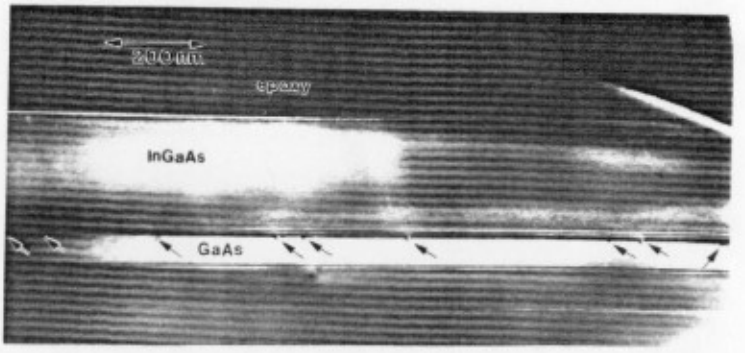

Fig. 3(a)

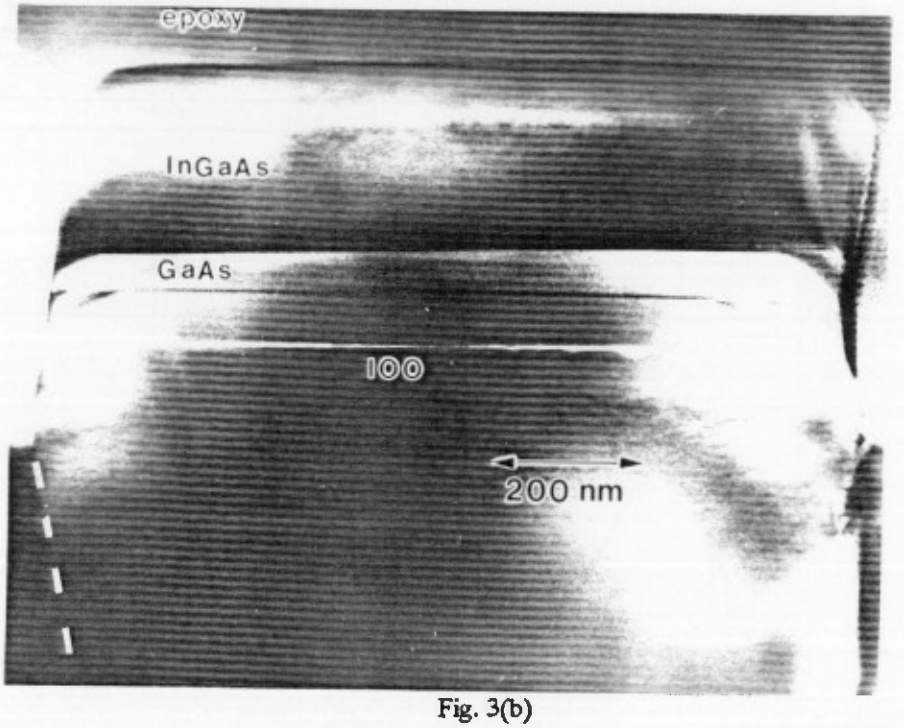

Fig. 3(b)

In Fig. 3(a) is shown a representative (200) dark field TEM micrograph showing a 2500Å thick $In_{0.11}Ga_{0.89}As$ growth in the unpatterned region. One observes a number of 60° interfacial misfit dislocations running parallel to the mesa length with a mean spacing of ~1500Å (indicated by arrows in the picture). Given that the thickness of $In_{0.11}Ga_{0.89}As$ layer is more than four times the nominal critical thickness, the presence of misfit dislocations is to be expected. Fig. 3(b) shows the same growth on a mesa with a width of ~1μm. By contrast, no misfit dislocations in the mesa region and running perpendicular to the mesa width can be seen at the interface. From areal measurements of the $In_{0.11}Ga_{0.89}As$ growth on the mesa and their comparison to the measured thickness of the $In_{0.11}Ga_{0.89}As$ layer

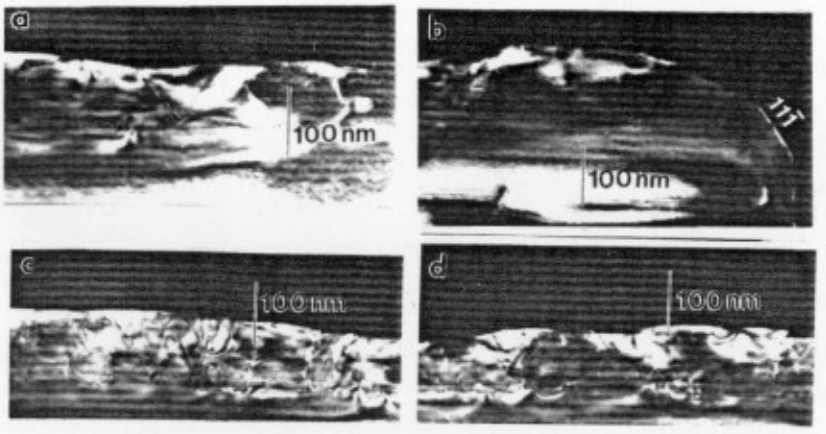

Fig. 4 (200) dark field cross-sectional TEM micro graphs showing the 1000Å $In_{0.25}Ga_{0.75}As$ growth on the central (a) and the edge (b) region of a mesa with width of ~1μm, the base region in between mesas (c) and the non-patterned region(d).

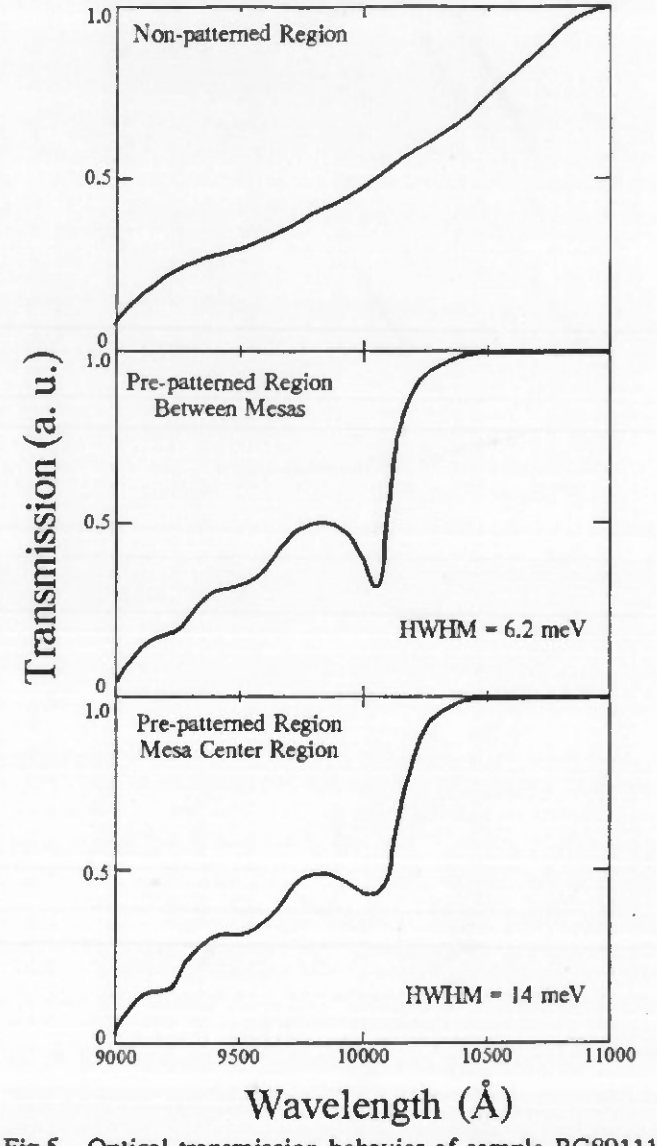

Fig.5 Optical transmission behavior of sample RG891110 for the MQW.

in the non-patterned region, we find that there has been no net migration of material between the mesas and the base region adjacent to them. Hence the mean alloy composition on the mesa is, within 1%, the same as that on the unpatterned region.

Similar studies with increasing x revealed that at x~ 0.25 the critical thickness for dislocation generation saturated at the unpatterned substrate value of ~130Å for mesas down to 1μm width. This is illustrated in Fig. 4 and provides an important guideline to the growth of MQWs for the purpose of examining their absorption and electroabsorption behavior as discussed next.

We now turn to the behavior of MQWs grown on patterned GaAs(100). In Fig. 5 is shown the optical behavior of sample number RG891110 which consists of 100 periods of $In_{0.20}Ga_{0.80}As$(28ML) /GaAs(56ML) grown on a patterened GaAs(100) substrate. Both the unpatterned region and the patterned region (mesa size of 16x18μm and pitch of 40μm) were studied. The total thickness of the MQW is (79.24Å +158.48Å) x 100 = 2.377μm, not accounting for the elongation in $In_{0.20}Ga_{0.80}As$ layers brought on by the Poisson effect. Estimation of the critical thickness of such a multilayered structure made from a combination of the theory for a free standing MQW[1] and any one of the prevalent expressions for an epilayer on a

substrate given in references 2 and 3 give values ranging from 153Å to 5251Å. The transmission spectra were measured using a collimated beam obtained from a 50W tungsten halogen lamp with a 100x microscope objective lens. The beam size on the sample was 2 to 3μm. A SPEX 1704 monochromator with slit setting for 2Å and a LN_2-cooled Ge detector was used for detection. The spectra were normalized to the system response. The unpatterned region shows no excitonic features, indicating a high density of defects in the active region. By contrast, the MQWs growth on top of the mesas and in between the mesas show not only the usual heavy hole (hh) to first confined electron (1e) excitonic transitions at ~1μm wavelength, but even the light hole (lh) to 1e and second hh to second electron excitonic features are resolved, indicating the high quality of the MQW and low defect density in these regions. The HWHM of the exciton (hh-1e) for the MQW in the region between the mesas and on top of the mesa are 6.2meV and 14meV, respectively. The assignment of the excitonic features is based on good agreement with calculations carried out within the usual effective mass approximation and accounting for the strain[9].

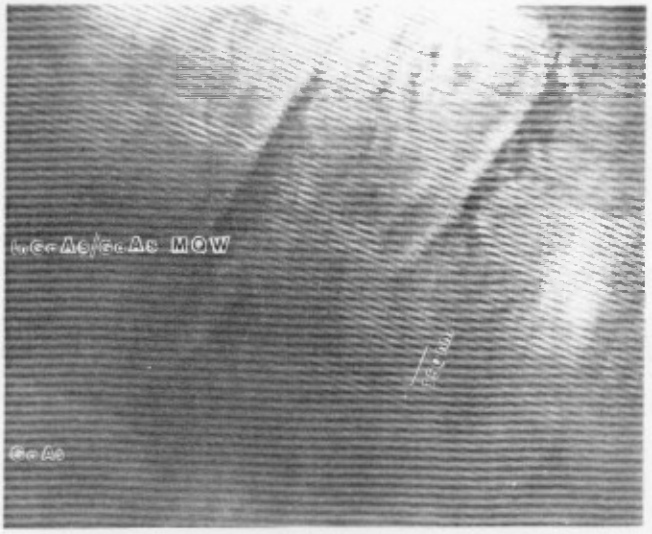

Fig. 6(a)

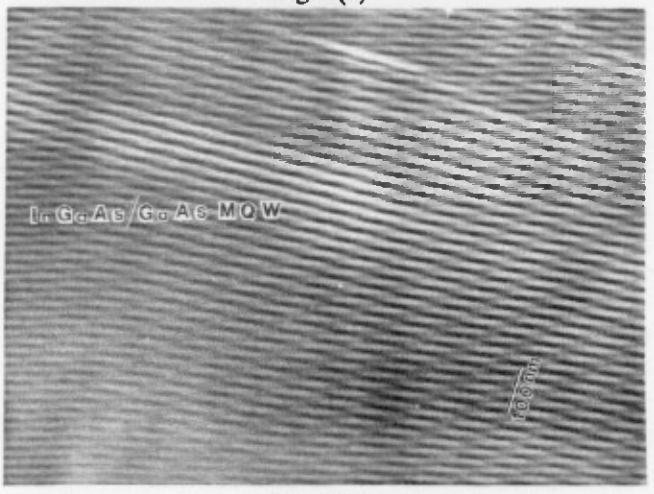

Fig. 6(b)

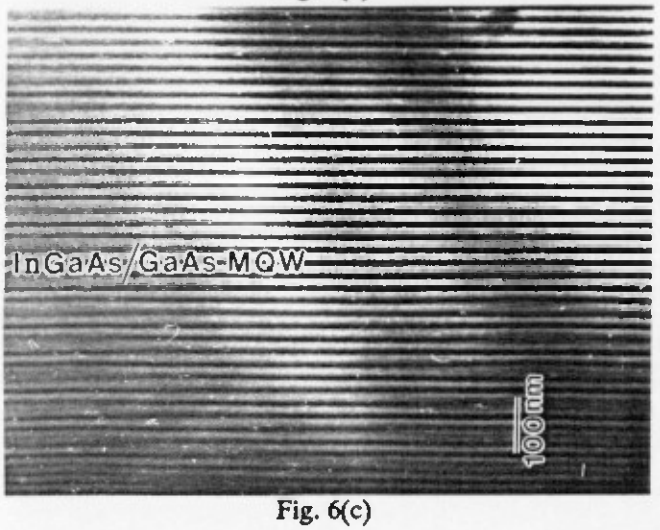

Fig. 6(c)

The higher quality of the transmission behavior in the valley regions compared to the mesa top was unexpected and led us to examine the structural quality of the MQWs in the above discussed three regions.

In fig. 6(a) is shown a TEM image contrast taken with the electron beam along the [1$\bar{1}$0] azimuth for a specimen prepared from the unpatterned region. As expected a large number of structural defects, including threading dislocations, are present throughout

the MQW structure. Fig. 6(b) shows the corresponding image contrast picture taken from the central area of a mesa in the patterned region. In the growth direction, the region shown corresponds to the middle region of the ~2.4μm thick MQW. Remarkably perfect $In_{0.20}Ga_{0.80}As$ (dark) and GaAs (light) layers are visible with hardly any evidence of structural defects at the level of the TEM resolution. The same was found all the way from the region down at the MQW substrate interface to the top of the MQW. Several mesas were examined and the results were the same. However, towards the edges of the mesas, the layering was found not to be good within 2μm to 3μm of the edges even though no defects were visible using the customarily chosen [$1\bar{1}0$] azimuth. The presence of contiguous mesa top plane, sidewall planes (typically (111) with some high index facets such as {311}/{411}, {11,1,1} etc) gives rise to interfacet cation migration whose degree and nature is sensitive to the growth conditions, as we have previously demonstrated[11]. We therefore suspect that interfacet migration is in part, if not largely, responsible for the degradation of the sharpness of layering near the edges of the mesas. The mesa region was further examined employing the ($\bar{2}20$) reflection with the electron beam along the [$1\bar{1}1$] azimuth since the optimum conditions for layer image contrast and examination of the defects are not necessarily the same. A defect linear density $\leq 10^5 cm^{-1}$ is found. Finally, in fig. 6(c) is shown the TEM image contrast taken from the valley region between the mesas with the electron beam along the [110] azimuth. Once again, no defects are visible and, at the level of TEM resolution, the valley region appears as good as the central regions of the mesas. The combined optical and structural behavior thus indicates that the excitonic features are more sensitive to the structural quality than the resolution of the TEM.

These results were reported in publications 4 through 6 noted in section IV.

III.A2 Influence of Strain Induced Deep Level Defects, Dielectric Encapsulation and Rapid Thermal annealing

The role of strain induced deep level defects (point complexes and dislocations) in influencing the excitonic absorption and electro-absorption had not been examined prior to the studies undertaken under this contract and summarized in the following. However, it is to be expected that deep levels associated with strain-induced defects will impact the electro-absorption behavior and that this is an important aspect of the optical properties of strained MQWs. Likewise, in most cases, completion of the pixellated device structure requires deposition of an isolation dielectric such as Si_3N_4. The same is, in fact, necessary in many cases to examine the intrinsic nature of the electroabsorption since application of the reverse bias can otherwise be limited by current leakage paths on exposed mesa surfaces due to contamination. Deposition of a dielectric however then raises its own associated concerns as to its influence on the optical characteristics of the MQW structure, particularly when it is strained. For these reasons, during the course of the previously noted investigations of the strained InGaAs/GaAs

MQW structures the results suggested that these aspects needed to be examined to avoid confusion between intrinsic and extrinsic influences on their optical properties. Consequently, some effort was spent on these aspect even though it was not originally intended.

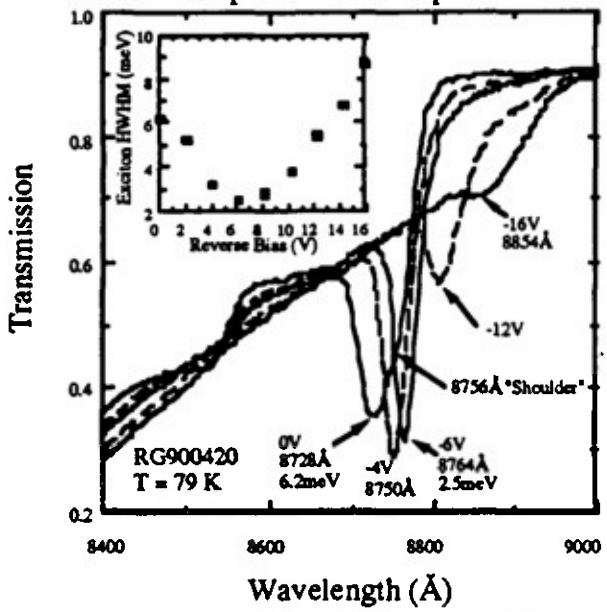

Fig. 7 The LN_2 temperature electro-transmission behavior of sample RG900420. The inset shows the exciton HWHM as a function of applied bias.

It has been known that shallow dopants in multiple quantum wells cause the observed exciton feature to broaden monotonically with increasing bias[12]. By contrast, we observed also an unusual phenomenon of the initial narrowing of the free exciton absorption linewidth with applied reverse bias in a GaAs/InGaAs MQW grown in a p-i(MQW)-n structure. Fig. 7 shows the LN_2 temperature electro-transmission behavior of a sample (RG900420) which consists of n^+ GaAs (100) substrate, Si doped ($5 \times 10^{18}/cm^3$) n^+ GaAs buffer, 50 period undoped $In_{0.11}Ga_{0.89}As$ (100Å)/GaAs(200Å) MQW structure, and a 2000Å thick Be doped ($2x10^{18}/cm^3$) p^+ GaAs cap layer. At zero bias, the excitonic feature is seen at 8728Å (1.4201eV) and a "shoulder" can be observed at 8756Å (1.4156eV). From a separate PL measurement, the shoulder is identified to be from the QWs adjacent to n^+ buffer layer. The strongest absorption occurs at a reverse bias of -4V where the excitonic feature becomes sharper. The half-width at half-maximum (HWHM) however reaches its minimum value of 2.5 meV at -6V (inset of fig.7) although the absorption is seen to decrease because of the loss of the oscillator strength. The absorption decreases further at higher reverse bias and the excitonic absorption is tunnel-broadened.

The usual charge transfer associated with *shallow* impurities cannot explain this line narrowing phenomenon[12]. Through a systematic examination of the sample behavior using electro-transmission, electro-photoluminescence, capacitance-voltage profiling and transmission electron microscopy we determined that this unusual narrowing is related to the strain-induced deep electron traps located in the nearby i(MQW) region. Under a reverse bias, as these deep levels in the MQW are lifted above the Fermi level of the n region, the trapped charges increasingly return to the n doped buffer layer. The band bending concommitantly decreases, and the exciton line becomes narrower until full depletion is reached. Fig. 8 shows the 5K photoluminescence behavior of this sample at zero bias taken under Ar^+ laser illumination. A strong and highly symmetric excitonic feature was observed at 8701Å (1.4245eV). The full width at half maximum of this

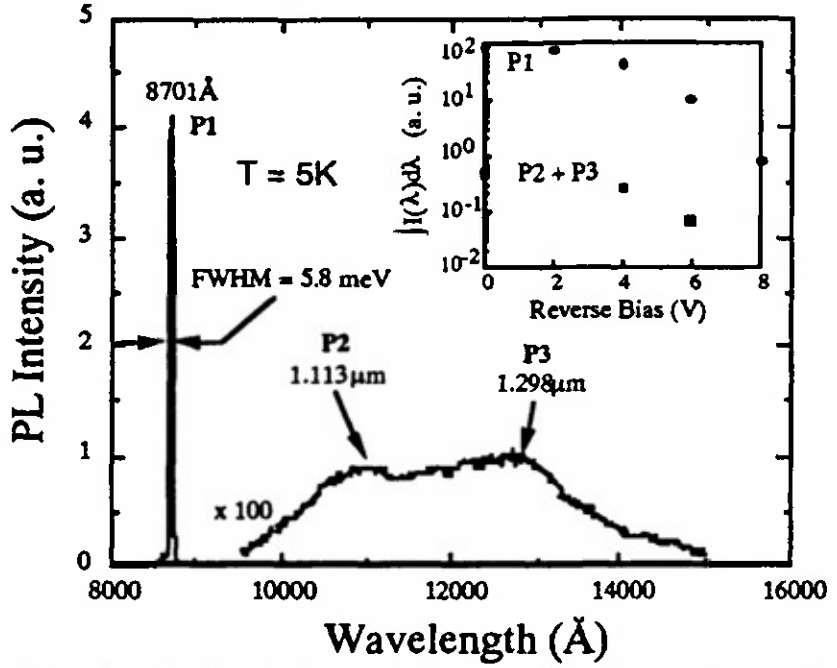

Fig.8 5K photoluminescence spectrum showing the existence of deep defects. The inset shows the integrated PL intensity as a function of bias.

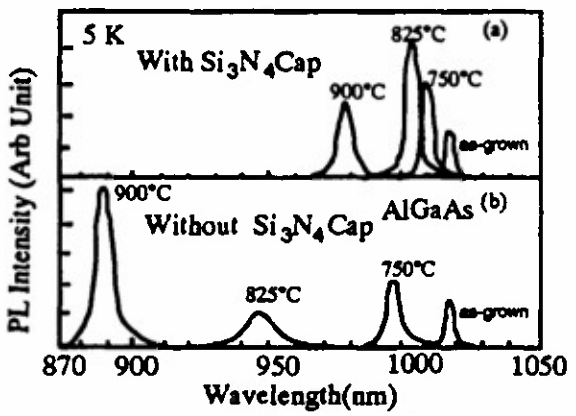

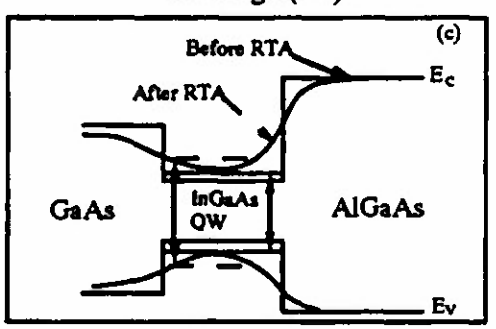

Fig. 9 Behavior of the 5K photoluminescence spectra of GaAs / $[In_{0.35}Ga_{0.65}As)_{15}(GaAs)_4]_3/[(AlAs)_5(GaAs)_2]$ SQW as a function of the RTA temperature for both as-grown and Si_3N_4 encapsulated specimens

feature is 5.8meV. Two defect related features were observed at 1.113μm (1.114eV) and 1.298μm (0.955eV). All these features were identified to be from the i-region because they quench under an applied bias (see inset in Fig.8). The defect related features quench at the same rate as the exciton. It should be noted that the features observed in the PL are from the top few wells close to p cap layer and only radiative defects are observed. Nevertheless, the PL revealed deep defect related emission from the strained MQWs not observed in the p^+ cap layer.

Finally, fig. 9 shows an illustrtive example of the influence of Si_3N_4 on the exciton behavior of strained single quantum well. Deposition of the silicon nitride is found to induce a small blue shift in the exciton peak, as can be seen by comparing the "as-grown" peaks in Fig. 9(a) and (b). Rapid thermal annealing induces a further blue shift, though not as large as that induced in the unencapsulated (i.e. as-grown) structures. The RTA induced changes indicate inter-diffusion of the group III atoms at the GaAs / InGaAs and InGaAs / AlGaAs interfaces, as illustrated in Fig. 9(c).

These results were reported in publications 3 and 7 noted in section IV.

III.B VERTICAL TRANSPORT: RESONANT TUNNELLING DIODES

Besides the optical characteristics of thick MQW structures involving strained InGaAs/GaAs wells, another set of studies undertaken under this contract examined the vertical transport behavior in highly strained InGaAs/AlAs based resonant tunneling diodes. These studies were, in part, a continuation of the transport studies in the lattice matched GaAs/AlGaAs system undertaken in the immediately preceding ARO contract. Their connection to the studies of strained single and multiple quantum well structures on unpatterned and patterned GaAs(100) substrates arises from the same common thread, namely establishing the limits on the advantages to be had via growth on prepatterned mesas. As single epilayers and quantum wells are the first two stages of work leading to multiple quantum wells necessary for studies of the optical absorption characteristics, the single quantum findings also served to provide both the platform and the opportunity to examine the transport characteristics - both parallel and perpendicular (i.e. vertical) to the interfaces. However, under this contract the studies were limited to vertical transport and in particular to the behavior of resonant tunneling diodes. Consequently, in the following we provide a summary of the essential findings.

Use of $In_xGa_{1-x}As$ wells and AlAs or AlSb barriers in resonant tunneling diodes (RTD) takes advantage of the higher conduction band-edge discontinuity (ΔE_C) and thereby cuts down the non-resonant currents. We demonstrated a way of improving the peak-to-valley ratio (PVR) in these structures through use of the lower bandgap pseudomorphic $In_xGa_{1-x}As$ spacers leading to a **triple well-double barrier structure** as illustrated in Fig. 10.

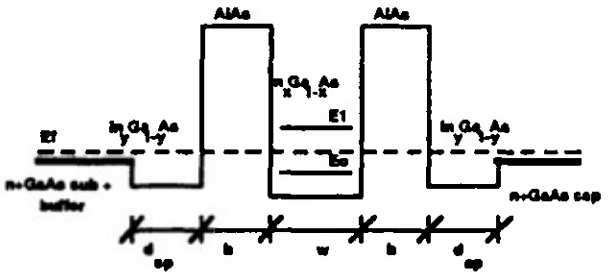

Fig. 10

The high In content dictated by the need for high ΔE_C gives rise to two severe difficulties; (i) for x ~0.5, the critical thickness for misfit (~3.5%) induced defect formation is ≤ 10 monolayers (ML) for the individual layer itself, and (ii) the large difference in the congruent evaporation temperatures of InAs (380°C), GaAs (650°C) and AlAs (850°C) imposes severe constraints on finding growth conditions suitable for the growth of both AlAs barrier and $In_xGa_{1-x}As$ well layers. Perhaps even more significant a fact revealed in examinations of the kinetics of growth is that growth of an alloy under strain is far more difficult than a binary compound for the same degree of strain. This is a consequence of the differing influence of strain on the migration, reaction and evaporation kinetics of the two components, In and Ga in the present case. Consequently, new approaches to minimising the deleterious effects of strain need to be sought if the $GaAs/In_xGa_{1-x}As$ system is to be fruitfully exploited. We realized a room temperature PVR of 4.5, employing the triple well - double barrier RT structure and pushing the well layer In

content to 25% which was the best reported at that time. This is a 40% increase in PVR over a 10% In structure and is a combined consequence of a 10% increase in the peak current and a 20% decrease in the non-resonant valley current. Both are a consequence of the ground and first excited states (E_0 and E_1) of the well moving down in energy with respect to the Fermi energy in the injecting n^+ GaAs as the conduction band discontinuity increases with increased In content. In the RTD structure, the spacer closer to the substrate is 9 monolayers (ML) i.e. 25.5Å thick, while the one on top is 20ML thick. The well, lower barrier, and upper barrier thicknesses are 18ML, 11ML, and 11ML respectively. Hence, we have compared the RTDs grown on an unpatterned region and on a pre-patterned region containing 20 μm x 20 μm square, 1 μm deep mesas in order to achieve strain relief of the lattice mismatched layers at the mesa edges. After growth both structures were processed into 12 μm x 12 μm mesas for test. A typical PVR of 4.2 (best device showed 4.5) at 300K and 15 at 77K was achieved with a J_p of 11kA/cm^2 at 300K and 13kA/cm^2 at 77K. The characteristics of the devices on the unpatterned and pre-patterned regions showed identical results. Transmission electron microscope studies of various regions of the unpatterned and patterned parts showed absence of misfit dislocations in both of these regions and equally high quality interfaces.

We have pushed further the In content to 0.3. An RTD consisting of $In_{0.3}Ga_{0.7}As$ spacer (20ML)/AlAs barrier (9ML)/$In_{0.3}Ga_{0.7}As$ well (23ML)/AlAs barrier (9ML)/$In_{0.3}Ga_{0.7}As$ spacer (20ML) and grown at 555°C showed very weak negative differential resistance (NDR) in the pre-patterned region and no NDR in the unpatterned region. Fig. 11 shows a (200) dark field cross-section image of the structure. The bright layers are the AlAs barriers and the darkest layers are the $In_{0.3}Ga_{0.7}As$ layers. Clearly, Stranski - Krastanov growth mode had set in before the first spacer layer growth was complete. Attendant with this is a large number of threading dislocations whose density is around $5x10^9/cm^2$. The growth temperature was obviously high enough to encourage strong interplanar migration. A second RTD was then grown at a lower temperature of 425°C with a $In_{0.3}Ga_{0.7}As$ spacer (16ML) / AlAs barrier (8ML) / $In_{0.3}Ga_{0.7}As$ well (18ML) / AlAs barrier (8ML) /$In_{0.3}Ga_{0.7}As$ spacer (16ML) structure. The growth temperature was however kept at 525°C during the growth of the AlAs barriers. The cross-sectional (200) dark field image of this sample (Fig. 12) shows that by cutting down the growth temperature one has succeeded in maintaining a 2-D layer-by-layer growth mode and the entire structure

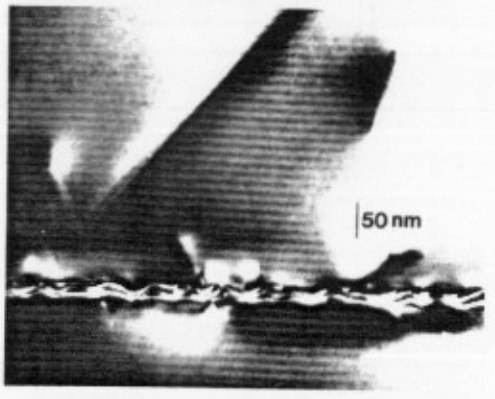

Fig. 11

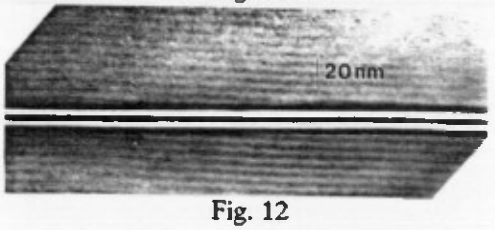

Fig. 12

is smooth and continuous. The somewhat smaller thickness of the $In_{0.3}Ga_{0.7}As$ layers we believe does not account for the drastic change in morphology observed since for the earlier sample (grown at 555°C), it is quite clear from the TEM micrograph (and also observed in RHEED during growth) that the 3-D islanding had set in before the first spacer layer (thickness 20 ML) growth was completed. Attendant with this smooth morphology, the TEM analysis shows a reduction in the defect density itself. No defects were observed in the cross-sectional studies: the defect density therefore is $<10^7 cm^{-2}$ in this sample. The electrical characteristics show strong resonant tunneling behavior. The room temperature peak to valley ratio is 5.2 at a peak current density of $32kA/cm^2$. This was the the best result reported at that time for alloy $In_xGa_{1-x}As$ /AlAs based RTDs grown on GaAs substrates.

These results were reported in publications 8 through 10 noted in section IV.

III.C GROWTH ON GaAs(111)B AND REALIZATION OF THREE DIMENSIONALLY CONFINED STRUCTURES VIA ONE-STEP GROWTH PROCESS

Realization of semiconductor heterostructures that are also confined in the growth plane (i.e lateral directions) on sub 100nm length scales is a subject attracting much attention. *Two* dimensionally confined structures (i.e wires) on nonplanar patterned GaAs (100) have been realized[13] by exploiting the behavior of GaAs growth at the bottom of V-shaped valleys between long mesas (ridges). The particular aspect of growth on nonplanar patterned substrates that we exploit is, however, a bit different in its approach and offers wider applicability. It is, in fact, an approach employed earlier[14] to realize confinement in one lateral direction (i. e. wire-like structures) via growth on top of mesas on GaAs (100). We refer to this approach as the **substrate encoded size reducing epitaxy (SESRE)**. Utilizing the SESRE approach we have achieved the first realization of *three*-dimensionally confined structures (i.e. boxes) via growth on nonplanar patterned GaAs(111)B substrates.

The potential advantages of the *in-situ* one-step growth controlled approaches to realization of laterally confined structures over the more traditional approaches that employ post-growth processing to achieve pixels of nanostructure dimensions lie in the ability, in principle, to minimize contamination and processing induced surface and subsurface damage faced in the traditional approaches. These potential advantages however come at the cost of increasingly complex growth control. Nevertheless, the *in-situ* growth approaches offer a class whose potential is worth assessing, along side the post-growth processing approaches. The particular objective of the SESRE approach is to find growth conditions such that the attendant migration kinetics of the impinging species during growth lead simultaneously to (i) either preservation of an appropriately chosen as-patterned shape or self-generation, via growth, of appropriate new facets, and (ii) reduction in the mesa top size. If such could be achieved then the as-patterned

mesa size can be *intentionally* kept significantly (an order of magnitude) larger than the eventually desired nanostructure size scale. Then, via a buffer layer growth, it can be reduced to the desired nanostructure size regime to create, *in-situ*, an array of templates suited for the growth of the quantum well nanostructures.

To fully exploit the potential of such approaches an understanding of the driving forces contributing to the direction of migration is the key. We have offered a framework based upon the atomistic structural and chemical nature of the facets involved and the relative competition between the driving forces arising from the electronic energies of stepped surfaces and the chemical potential gradient induced by the incident flux. The tendency for migration from the {311} side walls to the (100) mesa top was thus encoded by choosing the patterning direction such that the As dangling orbitals on the side facets are parallel to the direction of the ridge and thus the repulsive nature of the ledge-ledge interaction energy[15] provides a driving force opposite to the incident flux induced built-in direction of the chemical potential gradient from the mesa top towards the side wall. Under appropriate growth conditions then the net direction of migration was made to be from the side walls to the mesa top. We note that choosing a patterning direction such that the As dangling orbitals on the (100) mesa top are perpendicular to the ridge direction does not permit encoding the desired {311} side facet to (100) mesa top direction of interfacet migration due to the attractive ledge-ledge interaction energy[15] acting in concert with the direction of chemical potential gradient. This is manifest in the work of Smith *et al* [16] and Mannoh *et al* [17] which observed laterally expanding mesa top for patterning along such a direction. Evidently, the ability to realize appropriate directionality of migration is thus tied to an appropriate choice of the mesa shape, the atomic nature and orientation of the orbitals and control of chemical potential gradients via choice of growth conditions. Hence we refer to such a process as substrate encoded size reducing epitaxy (SESRE).

Essentially all the work reported to date following this one-step *in-situ* appoach has been restricted to the realization of structures with confinement in the growth plus one lateral direction i. e. quantum wires. This is a consequence of the use of (001) substrates (singular or vicinal). Due to the lack of a higher order symmetry element perpendicular to (001), simultaneous size reduction along more than one lateral direction required for the fabrication of quantum boxes (i.e. 3D confined structures) appears, at best, to be difficult on the (001) orientation, although there has been at least a report[18] of having overcome the symmetry problem. The {111} surface on the other hand, has a 3-fold axis of symmetry perpendicular to the surface and thus offers the possibility of realizing *three*-dimensionally confined structures via a one-step growth process on pre-patterned nonplanar substrates containing laterally bounded pyramidal mesa shapes that offer the ability to encode the direction of interfacet migration and thus achieve size reduction in both lateral directions during growth. For this reason the GaAs(111)B orientation was chosen in this

work. As growth on even the planar (i.e. unpatterened) GaAs(111)B surface had not been successful prior to our work, such growth was examined and brought under control first. The discussion that follows thus first discusses growth on unpatterned GaAs(111)B and then growth on patterned GaAs(111)B.

III.C1 GaAs Homeopitaxy & Growth Control

The first problem encountered in molecular beam epitaxical (MBE) growth on GaAs(111)B is the surface morphology of the grown layer. The grown surfaces are found to be easily marred by pyramid-like structures first reported by Cho[19]. Twins[20] are also easily formed during growth. The early work of Cho et al found some growths with no pyramids but with surface striations on nominally non-misoriented substrates[19]. Good surface morphology has been realized recently using tilted (111)B GaAs substrates[21] via conventional MBE, or via migration enhanced epitaxy (MEE)[22] on non-misoriented substrates. An effective and reproducible way to control the usual MBE growth on the commonly employed GaAs(111)B±0.1° substrates had not been achieved prior to our work under this contract. We succeeded in the first such growth control via real time monitoring of the specular beam intensity in RHEED from static and dynamic GaAs(111)B surfaces. GaAs epilayers, twin free and with specular surface, were thus realized on non-misoriented GaAs(111)B via conventional MBE, using the optimized growth parameter space identified in terms of the starting surface phase diagram and the temporal behavior of RHEED specular beam intensity. The growth conditions, namely, arsenic pressure and substrate temperature for a certain growth rate, resulting in mirror-like grown surface morphology were found to lie in a narrow zone in the surface phase diagram defined by the RHEED intensity measurements. The temporal variation of the RHEED specular beam intensity was used to monitor the growth in real time. Since these are inherent characteristics of the surface and independent of specific growth machines and monitoring gauges, they can be generated for each growth system thus enabling reliable and reproducible growths on GaAs(111)B substrates.

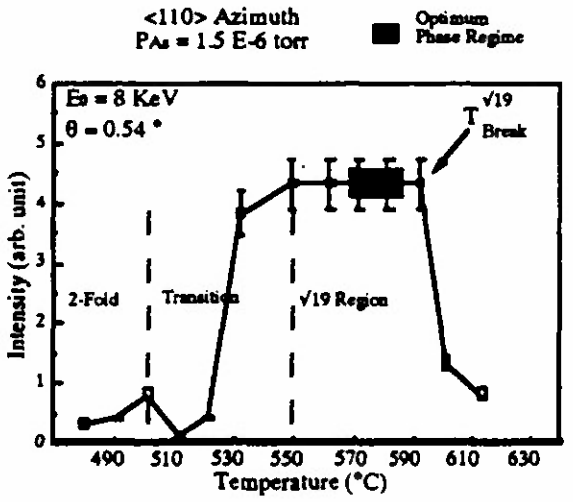

Fig. 13 Static RHEED specular spot intensity (I_0) variation with substrate temperature.

Fig. 13 shows the RHEED specular beam intensity (I_0) dependence on the substrate temperature(T_S) for a static (i.e. no growth) GaAs(111)B surface at a constant As_4 pressure. It can be used as an indicator of the surface phase due to the dramatic changes in the intensity at the phase boundaries. This also allows more precise measurement of the

boundaries of surface reconstructions than is possible by visual observation of the RHEED pattern . As expected, increasing arsenic pressure pushes the curve towards higher temperatures. The plot of the temperature surface phases as a function of arsenic pressure then gives the static surface phase diagram as shown in Fig.14.

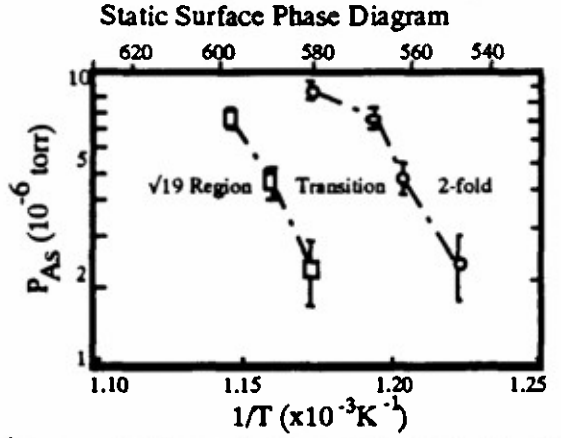

Fig.14 Variation in the temperature edges of surface phases with arsenic pressure.

The surface morphology was examined by using the static surface phase diagram as a guideline. The growth rate was kept fixed at around 0.3 ML/sec. All films grown under substrate temperature and arsenic pressure combinations which corresponded to the static surface having the 2-fold reconstruction had surfaces marred with triangular surface features associated with bulk twin of the density of the order of $10^7/cm^2$ and surface pyramids which usually overlapp one another making an estimation of their density difficult. Films grown under conditions corresponding to the static surface being in the transition regime had a lower density of twins and surface pyramids each of the order of $10^6/cm^2$. Films grown with the static surface near the low temperature edge of the intensity plateau corresponding to the √19 reconstruction does not show any bulk twin features but still has pyramids. Film grown at 10°C-30°C below the $T_{\sqrt{19}}^{break}$ point indicated in Fig.13. completely devoid of macroscopic surface features and is thus mirror-smooth.

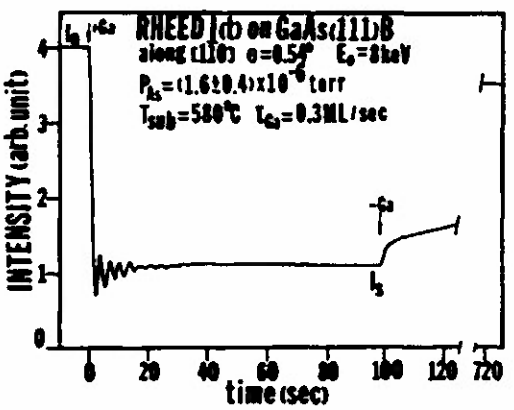

Fig. 15

Fig. 15 shows the temporal variation in the specular spot intensity during growth (dynamic RHEED) of a specular-surface film. The average intensity remained constant through out the growth and the intensity rapidly increases upon the termination of the growth. Growths which did not have these characteristics resulted in films with surfaces marred with macroscopic features. The nature of the dynamic RHEED can thus be used to *monitor* the macroscopic surface morphology of a growing film in real time.

It should be noted that the application of RHEED intensity measurements to growth control mentioned above is based on a systematic study of the nature of RHEED specular beam

intensity, namely, the relation between the surface atomic structure, morphology and the beam intensity behavior.

These results were reported in the publications 11 through 14 noted in section IV.

III.C2 Laterally Confined Growth

Crystalline semiconductors have long been known to exhibit differences in the chemical reactivities of the various crystallographic planes. These differences result in the preferential etching of certain planes over others in surface-reaction-rate limited wet etchants, most of which proceed by oxidation of the surface. The three-fold symmetry of the {111} surface as opposed to the two-fold symmetry of the (100) surface makes it reasonable to expect wet chemical etching of (111)B substrates to yield mesa profiles different from that observed on (100) substrates. We studied the etching behavior of GaAs (111)B and GaAs/AlGaAs (111)B multiple quantum wells grown on GaAs (111)B substrates and demonstrated the potential for realising laterally confined quantum wells with dimensions small enough to give rise to quantum confinement of the electronic states.

Fig. 16(a) is a scanning electron microscope (SEM) image of an array of mesas on an As terminated GaAs (111)B ($\pm$0.1°) substrate. The array was created by photolithographically defining an array of 5 μm square resist patterns aligned along a <110> direction followed by wet chemical etching. Fig. 16(b) is a magnified view of a typical mesa. Each mesa is a truncated triangular pyramid (in keeping with the 3-fold symmetry of the surface). The mesa top is (111)B and the three side facets are of the {100} type. The sides of the mesa top can be decreased from the initial pattern size all the way down to practically zero depending only on the duration of etching. Templates with arbitrarily small areal dimension can thus be created.

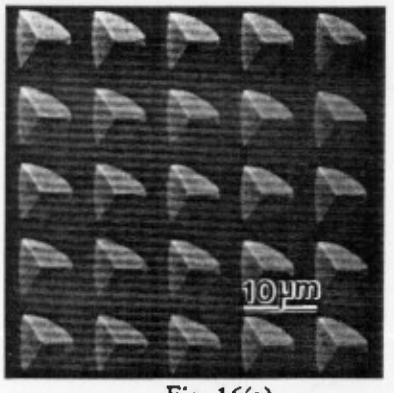

Fig. 16(a)

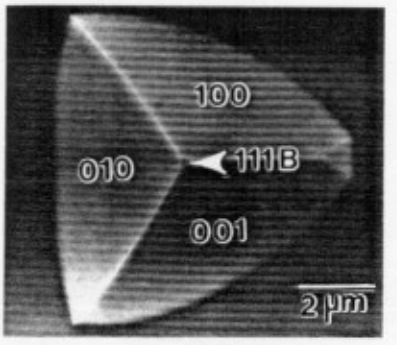

Fig. 16(b)

Fig. 17 is a TEM {200} dark field image of an etched mesa of a layered structure consisting of 13 periods 10 monolayer(ML) $Al_{0.3}Ga_{0.7}As$ / 40ML GaAs and finally a 10ML $Al_{0.3}Ga_{0.7}As$ / 20 ML GaAs capping layer. Etching was continued until the mesas pinched-off. It is worth noting that the imaged sample was *not* subjected to conventional TEM sample preparation techniques (i.e. mechanical polishing followed by ion thinning) in order to achieve

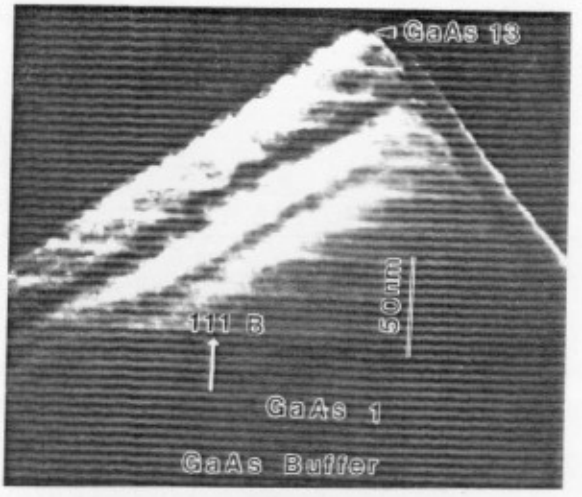

Fig. 17

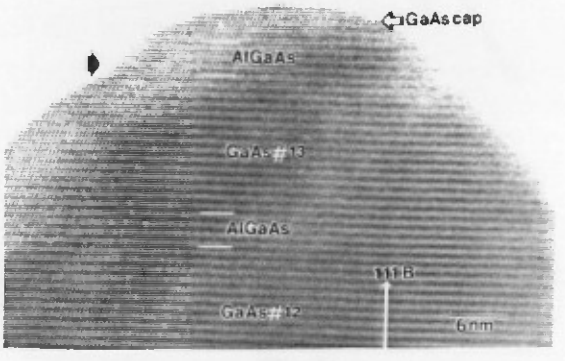

Fig. 18

electron transparency since the tips of the as-patterned mesas are thin enough to be electron transparent. The contrast from all 13 periods $Al_{0.3}Ga_{0.7}As$ (bright) barriers separating the GaAs (dark) wells can be seen. Fig. 18 is a <011> azimuth lattice resolved TEM image of a mesa showing the top three wells. The topmost AlGaAs layer is identied by the characteristic indentation at the left edge of the image caused by the difference in etch rates of GaAs and $Al_{0.3}Ga_{0.7}As$. Above this AlGaAs layer exists the last GaAs layer which corresponds to the capping layer of the grown structure. This last GaAs layer is measured to be about 12ML high and has a triangular base with 280Å long sides. This corresponds to a volume containing approximately $2.2x10^4$ atoms. The GaAs well #13 is a truncated pyramid 34 ML high with the length of the sides of the bottom triangle measuring 571Å and that of the top triangle measuring 329Å corresponding to a volume of $4.2x10^5$ atoms. These volumes compare favorably with quantum boxes estimated to contain $1.4x10^5$ atoms created on the (100) surface in the InGaAs/InP system via electron beam lithography followed by ion milling[23].

We now present our findings for the growth of *three*-dimensionally confined structures utilizing our SESRE approach on the GaAs (111)B substrates containing the pyramidal mesas shown in fig. 16. This is, in fact, the first effort to achieve *three* dimensional confinement via growth on nonplanar patterned substrates. The as-patterned substrate contained mesas with the sides of the triangular tops ranging from 0.5μm to 1.8μm. The growth sequence consisted of an initial 10ML $Al_{0.3}Ga_{0.7}As$ marker layer grown on the deoxidized surface, a GaAs buffer layer, an MQW consisting of 13 periods of 10ML $Al_{0.3}Ga_{0.7}As$/ 40ML GaAs followed by a 10ML $Al_{0.3}Ga_{0.7}As$/ 20ML GaAs cap. In Fig. 19 is shown a cross-sectional TEM image of a typical mesa. The initial AlGaAs marker layer determines the linear dimension of the as-patterned mesa to be 0.6 μm. The {200} dark field image clearly brings out the compositional contrast between the GaAs (dark) and AlGaAs (bright) layers. Besides the original (111)B plane, a new plane making a 19° angle with (111)B and identified to be of the {211} type has emerged during growth. The lateral dimension of the layers growing on the (111)B plane is seen to

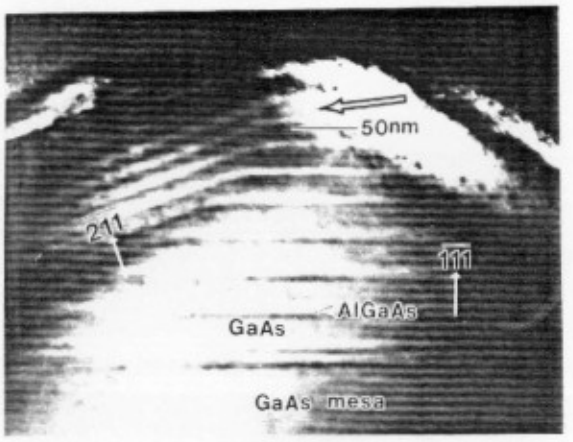

Fig. 19

monotonically *decrease* with growth under the growth conditions employed. After the 7th period of the MQW, the mesa top dimension has been reduced to about 500 Å. Deposition of the 8th GaAs layer (indicated in fig. 19 by a black arrow) pinches off the mesa, giving a laterally confined pinched-off GaAs pyramid of height ~130Å. This can be clearly seen in the profile of the 9th AlGaAs barrier layer of the MQW which has no segment parallel to (111). The remainder of the grown structure buries the pinched-off mesa.

The second sample is comprised of a 5 period multiple quantum well buffer made of 10ML $Al_{0.3}Ga_{0.7}As$ / 40ML GaAs, a nominal 60ML $Al_{0.3}Ga_{0.7}As$ / 40ML GaAs / 60ML $Al_{0.3}Ga_{0.7}As$ single quantum well (SQW), and finally a GaAs cap. Fig. 20(a) is a {200} dark field TEM image of the growth on a typical mesa top. The image clearly demonstrates the lateral finiteness of all layers on the mesa top. The mesa SQW lying along (111)B has a lateral dimension of approximately 2500Å. Fig. 20(b) is a magnified image of the quantum well showing its high structural perfection. As the laterally finite SQW was realized *in-situ*, the adverse influence of surface contamination faced in *ex-situ* patterning approaches is not expected to be faced here. This is evidenced by the cathodoluminescence (CL) results in Fig. 21. Fig. 21(a) is a spectral scan taken from a typical mesa top . The 8300 Å peak is attributed to bulk GaAs. The 7980 Å peak is from the SQW. Fig. 21(b) is a line scan at 7980 Å taken across the mesa. The 7980 Å intensity peaks at the mesa top indicating that the signal is coming primarily from the layers on the mesa top.

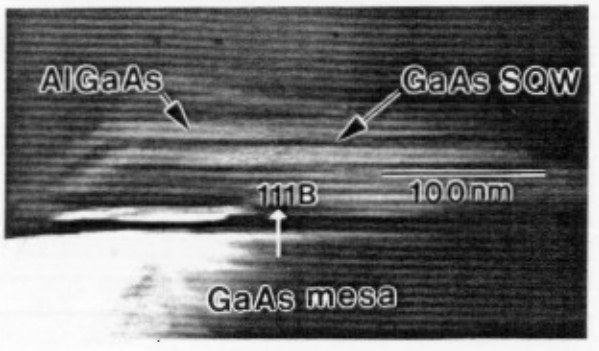

Fig. 20(a)

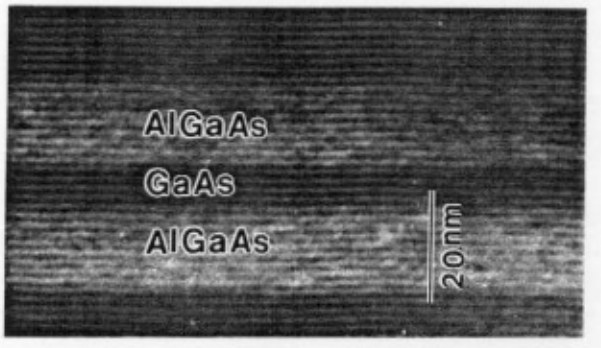

Fig. 20(b)

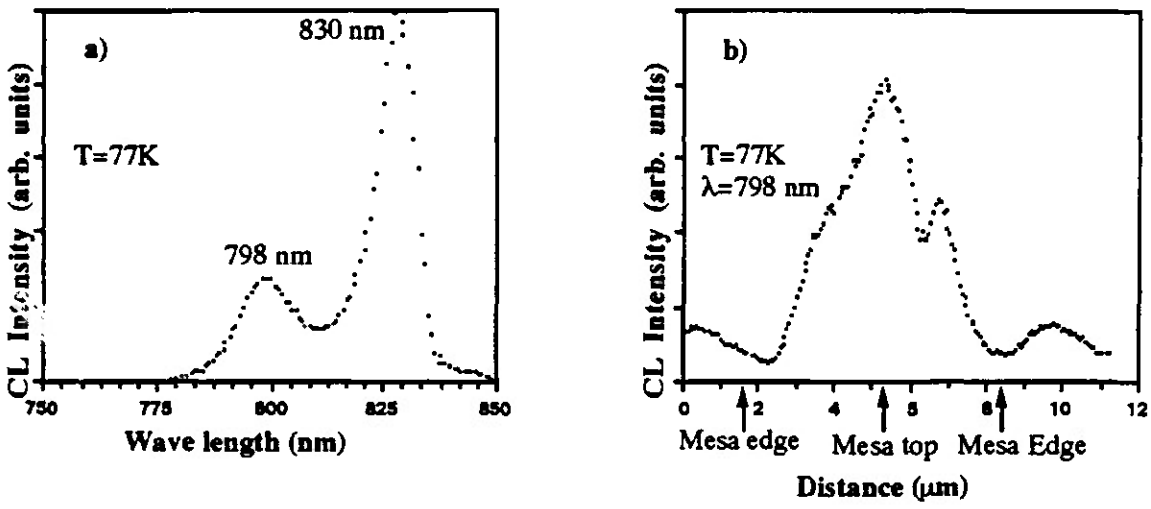

Fig.21 : (a) CL spectral scan taken from mesa top. (b) CL line scan at λ=798 nm taken across mesa

These results were reported in the publications 15 through 18 noted in the section IV.

III.D REFERENCES

1. J.W. Matthews and A.E. Blakeslee, J. Vac. Sci. Technol. **14**, 98(1977)
2. J.W. Matthews, S. Mader, and T.B. Light, J. Appl. Phys. **41**, 3800(1970)
3. A.T. Fiory,, J.C. Bean, L.C. Feldman, and I.K. Robinson, J. Appl. Phys. **56**, 1229(1984)
4 K. W. Jelly, R. W. H. Engelmann, K. Alavi, and H. Lee, Appl. Phys. Lett. **55**, 70 (1989); K. W. Jelly, K. Alavi, R. W. H. Engelmann, Electron. Lett. **24**, 1555 (1988).
5 M. Whitehead, P. Stevens, A. Rivers, and G. Parry, J. S. Robets, P. Mistry, M. Pate, and G. Hill, Appl. Phys. Lett., **53**, 956 (1988).
6. R. C. Miller, D. A. Kleinman, W. A. Nordland, Jr., and A. C. Gossard, Phys. Rev. **B22**, 863 (1980).
7. S. B. Ogale, A. Madhukar, F. Voillot, M. Thomsen, W. C. Tang, T. C. Lee, J. Y. Kim, and P. Chen, Phys. Rev. **B36**, 1662 (1987).
8. D. C. Bertolet, Jung-Kuei Hsu, K. M. Lau, E. S. Koteles and D. Owens, J. Appl. Phys. **64**, 6562 (1988).
9. Li Chen and A. Madhukar (unpublished).
10. P. Chen, J. Y. Kim, A. Madhukar, and N. M. Cho, Jour. Vac. Sci. Technol. **B4**, 890(1986)
11. S. Guha, A. Madhukar, K. Kaviani, L. Chen, R. Kuchibhotla, R. Kapre, M. Hyugaji and S. Xie, Proceedings of the MRS Symposium on "III-V Heterostructures for Electronic/Photonic Devices", Vol. **145**, P.27 (1989).
12. D. A. B. Miller, D. S. Chemla, T. C. Damen, A. C. Gossard, W. Wiegmann, T. H. Wood and C. A. Burrus, Phys. Rev. **B32** , 1043 (1985).

13. E. Kapon, D. M. Hwang, and R. Bhat, Phys. Rev. Lett., **63**, 430 (1989) and references to earlier work of the authors contained therein.
14. A. Madhukar, in The Physics of Quantum Electronic Devices, Ed. F. Capasso, Springer Series in Electronics and Photonics, Vol. **28**, p. 13 (Springer-Verlag, 1989)
15. D. K. Choi, T. Takai, S. Erkoc, T. Halcioglu, and W. A. Tiller, J. Cryst. Growth, **85**, 9 (1987)
16. J. S. Smith, P. L. Derry, S. Margalit, and A. Yariv, Appl. Phys. Lett., **47**, 712 (1985)
17. M. Mannoh, T. Yuasa, S. Naritsuka, K. Shmozaki, and M. Ishii, Appl. Phys. Lett., **47**, 728 (1985) ; also J. Appl. Phys., **62**, 764, (1987)
18. Y. D. Galeuchet, H. Rothuizen, and P. Roentgen, Appl. Phys. Lett., **58**, 2423 (1991)
19. A.Y. Cho J. Appl. Phys. **41**, 2780(1970)
20. K. C. Rajkumar, P. Chen and A. Madhukar, J. App. Phys. **69** 2219 (1991)
21. T. Hayakawa, M. Kondo, T. Suyama, K. Takahashi, S. Yamamoto and T. Hijikata Jap. J. App. Phys. **26** L302 (1987)
22. H. Imamoto, F. Sato, K. Imanaka, and M. Shimma, App. Phys. Lett. **55**, 115 (1989)
23. H. Temkin, G. J. Dolan, M. B. Panish, and S. N. G. Chu, Appl. Phys. Lett., **50**, 413 (1987)

IV. LIST OF PUBLICATIONS

The following publications are the result of full or partial support from ARO contract number DAA03-89-K-0170.

1. Li Chen, K.C. Rajkumar, A. Madhukar, W. Chen, S. Guha and K. Kaviani, "Realization of Sharp Excitonic Features in Highly Strained GaAs/$In_xGa_{1-x}As$ Multiple Quantum Wells Grown on GaAs(100) Substrates", Proc. of 6th International MBE Conference (Aug. 27-31, 1990, San Diego, CA), J. Cryst. Growth, **111**, 424 (1991).
2. Li Chen, K. Hu and A. Madhukar, "Behavior of Absorption Modulation in Highly Strained $In_xGa_{1-x}As$/GaAs Multiple Quantum Wells Grown via Molecular Beam Epitaxy on Patterned and Nonpatterned GaAs(100) Substrates", Mat. Res. Soc. **EA-21**, 317 (1990).
3. K. Kaviani, J. Chen, K.Z. Hu, L. Chen, and A. Madhukar, "Growth of High Quality Strained $Al_xGa_{1-x}As/In_{0.26}Ga_{0.74}As/Al_zGa_{1-z}As$ Quantum Wells and the Effect of Silicon Nitride Encapsulation and Rapid Thermal Annealing," J. Vac. Sci. Technol. **B10**, 793 (1992).
4. S. Guha, A. Madhukar and Li Chen, "Defect Reduction in Strained $In_xGa_{1-x}As$ via Growth on GaAs(100) Substrates Patterned to Submicron Dimensions", App. Phys. Letts. **56**, 2304 (1990).
5. S. Guha, A. Madhukar, Li Chen, K.C. Rajkumar and R. Kapre, "Interfacet Migration and Defect Formation in Heteroepitaxy on Patterned Substrates: AlGaAs and InGaAs on GaAs(100) in MBE", SPIE Proceedings on "Growth of Semiconductor Structures and High T_c Superconductors", Ed. A. Madhukar, Thin Films on Semiconductors, Vol. **1285**, P.160 (1990).
6. A. Madhukar, K.C. Rajkumar, Li Chen, S. Guha, K. Kaviani and R. Kapre, "Realization of Low Defect Density, Ultra Thick, Strained InGaAs/GaAs Multiple Quantum Well Structures via Growth on Patterned GaAs(100) Substrates", App. Phys. Letts., **57**, 2007 (1990).
7. L. Chen, W. Chen, K.C. Rajkumar, K.Z. Hu, and A. Madhukar, "Observation of the Influence of Strain Induced Deep Level Defects on the Electroabsorption Characteristics of InGaAs/GaAs(100) Multiple Quantum Well Structures and Implications for Light Modulators", MRS Symp. Proc. **240**, 621 (1992).
8. R. Kapre, A. Madhukar, K. Kaviani, S. Guha and K.C. Rajkumar, "Realization and Analysis of GaAs/AlAs/$In_{0.1}Ga_{0.9}As$ Based Resonant Tunneling Diodes with High Peak to Valley Ratios at Room Temperature, App. Phys. Lett. **56**, 922 (1990).
9. R. Kapre, A. Madhukar and S. Guha, "$In_{0.25}Ga_{0.75}As$/AlAs Based Resonant Tunneling Diodes Grown on Pre-patterned and Non-patterned GaAs(100) Substrates", IEEE Electron Device Lett, **11**, 270 (1990).

10. S. Guha, A. Madhukar, R. Kapre and K.C. Rajkumar, "Initial Stages of Molecular Beam Epitaxical Growth of Highly Strained $In_xGa_{1-x}As$ On GaAs(100)", Proceedings of MRS Fall 1990 meeting on "Symposium on Evolution of Thin Film and Surface Microstructure", Boston, Mass., MRS Proceedings, **519**, 202 (1991).
11. K.C. Rajkumar, P. Chen and A. Madhukar, "Studies of the RHEED Specular Beam Intensity Variations on MBE Grown GaAs(111)B Surface", Proceedings of the 20th ICPS Conference (Aug. 1990, Thessaloniki, Greece), Eds. E.M. Anastassakis, J. Joannopoulos, (World Scientific, Singapore), Vol.1, p.276 (1990).
12. P. Chen, K.C. Rajkumar, A. Madhukar, "Growth Control of GaAs Epilayers with Specular Surface Free of Pyramids and Twins on GaAs(111)B Substrates via Molecular Beam Epitaxy", Appl. Phys. Letts. **58**, 1771 (1991).
13. P. Chen, K.C. Rajkumar and A. Madhukar, "Relation between Reflection High Energy Electron Diffraction Specular Beam Intensity and the Surface Atomic Structure/Surface Morphology of GaAs(111)B", J. Vac. Sci. Technol. **B9**, 2312 (1991).
14. K.C. Rajkumar, P. Chen and A. Madhukar, "Reflection Electron Diffraction and Structural Behavior of GaAs/GaAs(111)B Grown via MBE", Proceedings of MRS Fall Meeting, Boston, Mass. Nov. 1990, MRS Symp. Proc. 208, 193 (1991).
15. K.C. Rajkumar, K. Kaviani, J. Chen, P. Chen, and A. Madhukar, "Nanostructures on GaAs(111)B via Photolithography", App. Phys. Letts. **60**, 850 (1992).
16. K.C. Rajkumar, K. Kaviani, J. Chen, P. Chen, A. Madhukar, and D.H. Rich, " *In-Situ* approach of three-dimensionally confined structures on patterned GaAs(111)B substrates," MRS Proceed, **263**, 163 (1992).
17. K.C. Rajkumar, K. Kaviani, P. Chen, A. Madhukar, K. Rammohan and D.H. Rich, "One-step *in-situ* quantum dots via molecular beam epitaxy," J. Crystal Growth (in press).
18. A. Madhukar, K.C. Rajkumar, and P. Chen, "An *in-situ* approach to realization of three-dimensionaly confined structures via substrate encoded size reducing epitaxy on nonplanar patterned substrates," submitted to Appl. Phys. Lett.

V. LIST OF ALL PARTICIPATING PERSONNEL

The following personnel have been supported by this contract for their work relating to this contract

Graduate Students:

1.	Ravindra M. Kapre,	Ph. D,	May, 1991
2	Supratik Guha,	Ph. D,	Dec., 1990
3.	Li Chen,	Ph. D,	Jan., 1993
4.	K.C. Rajkumar,	Ph. D,	May, 1993

Post-Doctoral Personnel

1	Ping Chen,	Jan.,'90 to May, '92

VI. REPORT OF INVENTIONS

None